The sums of $\sum\{s_j\}$ and $\sum\{s_k\}$ are obtained by cyclic permutation of the components of $\mathbf{k}$ and x. We obtain therefore

$$F_{xx}(110)=\frac{8|e_x(-|j,\mathbf{k})|^2}{C(\mathbf{k})}\cos(k_xR_0)\times[\cos(k_yR_0)+\cos(k_zR_0)]+(\text{cyclic permutations}),$$

$$F_{xy}(110)=-\left[\frac{16e_x(-|j,\mathbf{k})e_y(-|j,\mathbf{k})}{C(\mathbf{k})}\times\sin(k_xR_0)\sin(k_yR_0)\right]+(\text{cyclic permutations}),$$

$$F_{zz}(110)=F_{xx}(001)=\left[\frac{16|e_x(-|j,\mathbf{k})|^2}{C(\mathbf{k})}\times\cos(k_xR_0)\cos(k_zR_0)\right]+(\text{cyclic permutations}),$$

$$F_{xx}(000)=\left[\frac{16|e_x(-|j,\mathbf{k})|^2}{C(\mathbf{k})}\right]+(\text{cyclic permutations}). \quad \text{(A8)}$$

These are the required sums necessary in solving Eqs. (3) and (29).

PHYSICAL REVIEW VOLUME 185, NUMBER 3 15 SEPTEMBER 1969

Theory of Electron-Phonon Interaction and Defect-Center Optical Spectra*

JOHN T. RITTER† AND JORDAN J. MARKMAN
Illinois Institute of Technology, Chicago, Illinois 60616
(Received 9 December 1968)

An electron-lattice interaction potential is derived and applied to the calculation of defect-center optical-spectra line shapes. Results have been limited to a model in which the electron-lattice interaction involves band-mode phonons; local modes and eigenvector-in-band resonance effects have been neglected. Spectral line shapes are analyzed in terms of a per-mode Huang-Rhys factor S_j. S_j is given by the defect-center wave functions and the electron-lattice interaction potential. Calculations are presented for the two extreme cases: broad-band spectra, in which many phonons are excited, and spectra with detailed attendant phonon structure, in which only a few phonons are excited. The former computations are the half-width and effective lattice frequency of the NaCl and KCl F-center absorption and luminescence spectra, which agree reasonably well with experiments. The latter calculations are a measure of one-phonon contributions to line shapes of centers in NaCl, KCl, and LiF. For this, only part of S_j, the per-mode lattice factor L_j, was evaluated. Comparison of frequency distributions formed from L_j to attendant phonon spectra of various F-aggregate centers showed agreement as to position of major features in the spectra.

I. INTRODUCTION

SEVERAL papers have reported optical spectra from defect centers in ionic crystals which display zero-phonon and detailed attendant phonon structure.[1] Figure 1, an example redrawn from Pierce,[1b] shows the LiF R_2-center absorption spectrum. The lowest-energy spike, at 3.175 eV, is a zero-phonon transition line where the lattice vibrations have not been excited. The band to the high-energy side of this line involves the excita-

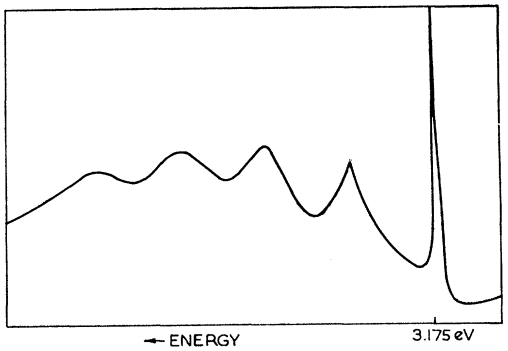

FIG. 1. Absorption spectrum of the R_2 center in LiF [from Ref. 1(b)].

* This paper is based on the thesis of JTR submitted to IIT in partial fulfillment of the requirement for the Ph.D. degree in Physics.

† Present address: University of Reading, Reading, England.

[1] Some papers reporting spectra with detailed attendant phonon structure are: F-aggregate centers in alkali halides: (a) D. B. Fitchen, R. H. Silsbee, T. A. Fulton, and E. L. Wolf, Phys. Rev. Letters **11**, 275 (1963); (b) C. B. Pierce, Phys. Rev. **135**, A83 (1964); (c) C. B. Pierce, *ibid.* **148**, 797 (1966); (d) D. B. Fitchen, H. R. Fetterman, and C. B. Pierce, Solid State Commun. **4**, 205 (1966). F-aggregate centers in MgO: (e) R. A. Shatas and G. A. Tanton, Bull. Am. Phys. Soc. **8**, 541 (1963); (f) R. D. King and B. Henderson, Proc. Phys. Soc. (London) **89**, 153 (1966). Impurity centers in ionic crystals: (g) G. F. Imbusch, W. M. Yen, A. L. Schawlow, G. E. Devlin, and J. P. Remeika, Phys. Rev. **136**, A481 (1964); (h) D. W. Langer and H. J. Richter, *ibid.* **146**, 554 (1966).

tion of lattice phonons accompanying the absorption of an optical photon. The positions of the additional spikes in this spectrum, relative to the zero-phonon line, are given approximately by $n\times(0.031$ eV), where $n=1$, 2, 3, and 4, corresponding to the creation of one, two, three, and four phonons. These spikes occur because phonons of about 0.031 eV are much more likely to be excited than those giving rise to the general background; i.e., the phonon sideband of a spectrum can be viewed as being a weighted distribution of the lattice vibration states that takes into account the probability of one- or many-phonon modes being excited by a transition of the center.

A rigorous calculation of spectral line shapes presents some formidable problems, since it is required to know the imperfect crystal-lattice vibrational states and the interaction between the lattice and the different defect-center electron states. However, experimental results for several centers indicate that a reasonably good description of the major features of their spectra may be calculated from a simplified model. Attendant phonon structure in spectra from different centers in the same crystal are often strikingly similar (e.g., compare the R_2 and M' LiF centers shown in Figs. 1 and 8 respectively), and the phonon frequencies associated with spikes in the spectra correspond to relatively large values of the host crystal's density of vibration states. This suggests that a starting point of a calculation of the attendant phonon structure might be to consider the interaction between an electron and the normal vibration modes of the host crystal. But the electron-crystal interaction must take into account the details of the lattice vibrations.

Several simplified approaches used in the past have been unsuccessful. One of these assumes that the electron-phonon interactions occur via the long-wavelength approximation to the longitudinal optical modes [see Huang and Rhys,[2a] Pekar,[2b] and Born and Huang[3] (p. 82)]. This assumes that all interacting lattice modes can be described by a single frequency. The concept holds for free electrons, as indicated from mobility measurements in alkali halides (see Markham,[4] p. 72), but it does not apply to point imperfections as established for the case of the F center (Ref. 4, Chap. X) and centers which have resolved fine structure. Furthermore, resolved structure shows that if the frequencies are weighted according to a Debye distribution, one obtains unsatisfactory results. Also, the host-crystal frequency distribution cannot be used directly since this will generally have peaks that are not present in the resolved structure.

In this paper we derive an electron-lattice scalar interaction potential that takes into account the actual details of the host-crystal lattice vibrations. The derivation follows Born-Huang's developement of the microscopic theory of optical dispersion for a medium of vibrating ions (Ref. 3, p. 328). The resulting interaction potential, derived in Sec. II, is linear in the lattice normal coordinates. The coefficient of a normal coordinate (a function of the electron position) determines the strength of the mode's interaction; collectively, the coefficients lead to predictions of spectral line shapes. This interaction potential does have some similarities with the "Fröhlich[5] interaction picture." By this phrase we mean the long-wavelength limit of the microscopic theory of Ref. 3 (hereafter referred to as BH). One of the best presentations of Fröhlich's idea is found in part I of BH, p. 82. This presentation is useful in the development of basic concepts, but can lead to erroneous results if not modified when actual calculations are carried through.

Section III discusses the eigenstates of the trapped electron-crystal system. By means of the Born-Oppenheimer technique, the imperfect lattice Hamiltonian is written in terms of the perfect crystal Hamiltonian, the electron-crystal potential terms, and the trapped electron wave functions. Section IV deals with the problem of calculating an optical-spectrum line shape from the system eigenstates. The case of a highly structured attendant phonon spectrum with a prominant zero-phonon line, in which only a few phonons are excited per optical transition, can be considered in a direct fashion: i.e., an expression is derived for the spectrum intensity in a small energy interval. For this direct calculation, we introduce the per-mode Huang-Rhys factor S_j. S_j is determined by the imperfection electron wave functions and the electron-lattice interaction potential. For the case of a broad-band spectrum, in which many phonons are excited by an optical transition, the direct line-shape analysis is not feasible with a general band-mode model. For this case some results of the method of moments are quoted. It is interesting to note that S_j remains a fundamental quantity describing the spectrum.

Section V presents specific calculations of many-phonon broad-band spectra and few-phonon spectra with detailed structure, both problems requiring estimation of the S_j. The former calculations consist of the temperature-dependent half-widths and effective lattice frequencies of the NaCl and KCl F-center absorption and luminescence spectra, computed from available wave functions and lattice vibration data. The latter calculations are limited to one-phonon contributions to the attendant phonon spectra. Since reliable wave functions for the discrete phonon centers are not known, we

[2] F-center calculations which use a Fröhlich (Ref. 5) electron-lattice interaction are: (a) K. Huang and A. Rhys, Proc. Phys. Soc. (London) **A204**, 406 (1950); (b) S. I. Pekar, *Untersuchungern über die Electronen Theorie der Kristalle* (Akademie-Verlag, Berlin, 1954) (English transl.: *Research in Electron Theory of Crystals*, M. S. S. E. C. tr. 5575).

[3] M. Born and K. Huang, *Dynamical Theory of Crystal Lattices* (Clarendon Press, Oxford, 1954).

[4] J. J. Markham, in *Solid State Physics*, edited by F. Seitz and D. Turnbull (Academic Press Inc., New York, 1966), Suppl. 8.

[5] H. Fröhlich, Advan. Phys. **3**, 325 (1954).

introduce and calculate a measure of S_j, the per-mode lattice factor L_j, which requires only lattice vibration data. Although phonon selection evidenced in an attendant phonon spectrum is expected to show dependence on the wave functions, the L_j alone, which do take some account of the electron-phonon interaction, can predict basic features of a spectrum. The calculations are compared to experimental spectra of various F-aggregate centers in NaCl, KCl, and LiF. Reasonable agreement is obtained between calculations and experiments for both the broad-band and highly structured spectra.

The theory and calculations presented here, dealing with basic features of phonon sidebands of ionic-crystal defect-center optical spectra, is of limited scope. Many relevant problems have not been considered. Also, some crude approximations, reviewed in Sec. VI, have been employed. Nevertheless, we feel that a basic understanding of the problems has been achieved. This results primarily from replacing concepts in part I of BH by more rigorous ones, so beautifully developed by Born in part II of BH.

II. TRAPPED ELECTRON-IONIC CRYSTAL POTENTIAL

The total potential function for a solid with an imperfection that has trapped one or more electrons can be written $V_T=V_P+V_I$, where V_P is the potential function for a perfect crystal and V_I is the potential, due to the presence of the imperfection, that must be added to obtain the true total potential. V_I will alter the normal modes of the perfect crystal deriving from V_P and account for the trapped electron-lattice interaction. The object here is to derive an electron-lattice interaction potential, which comprises an important part of V_I, under the special assumption that the major interaction is with normal modes which are primarily determined by the long-range lattice order. This interaction potential will be written in terms of the lattice vibration parameters. The perfect-crystal potential is first briefly described to define the notation and to introduce the required vibration parameters.

Forms of the Perfect-Crystal Normal Modes

BH develop the normal coordinates several times; their first development is in Sec. 15. This theory is completely general and has to be used in nonsymmetric structures such as molecules and point imperfections in solids. For our calculations the development in Secs. 24 and 38 is more useful since it utilizes the symmetry of the perfect lattice. Here we start with the development in Sec. 15 and end up with the normal modes described in Secs. 24 and 38.

Consider a portion of a crystal containing nN ions, where n is the number of ions in a cell and N is the number of cells. Let $u_\alpha(K)$ be the αth ($\alpha=x, y, z$) component of displacement of the Kth ion. Then, in the harmonic approximation, the potential function for this macrocell portion, apart from a constant, is given by the bilinear form

$$\Phi_2=\tfrac{1}{2}\sum_{K}^{nN}\sum_{\alpha}^{3}\sum_{K'}^{}\sum_{\alpha'}^{3}u_\alpha(K)\Phi_{\alpha\alpha'}(K,K')u_{\alpha'}(K'). \quad (2.1)$$

Generalized coordinates $Q(j)$ ($j=1, \cdots, 3nN$) can be found as linear combinations of the displacements $u_\alpha(K)$:

$$Q(j)=\frac{1}{\sqrt{N}}\sum_{K}e_\alpha(K;j)(\sqrt{M_K})u_\alpha(K) \quad (2.2)$$

(M_K is the mass of the Kth ion), such that Φ_2 takes on a diagonal form:

$$\Phi_2=\sum_{j}^{3nN}Q^*(j)\tfrac{1}{2}\omega^2(j)Q(j). \quad (2.3)$$

In principle, one could introduce the real normal coordinates q_j of BH, Sec. 15, here, but instead we introduce the complex ones of BH, Sec. 38. The ω's are the angular vibration frequencies. They are the $3nN$ solutions of the secular determinant.

$$|(M_KM_{K'})^{-1/2}\Phi_{\alpha\alpha'}(K,K')-\omega^2\delta_{\alpha\alpha'}\delta_{KK'}|=0. \quad (2.4)$$

The usual procedure of calculating a representative spectrum of $\omega(j)$ values employs periodic boundary conditions to a cubic macrocell of $N=L^3$ unit cells and uses the translational symmetry of the crystal to reduce the dimension of the problem of Eq. (2.4) from $3nN$ to $3n$. N distinct wave vectors $\mathbf{y}$ are introduced which are specified in reciprocal space by a triple index of integers h_1, h_2, and h_3:

$$\mathbf{y}(h)=(1/L)\{h_1\mathbf{b}_1+h_2\mathbf{b}_2+h_3\mathbf{b}_3\}, \quad (2.5)$$

where the $\mathbf{b}_i$ are reciprocal-lattice vectors defined in relation to the primary unit lattice vectors $\mathbf{a}_j$:

$$\mathbf{b}_i\cdot\mathbf{a}_j=\delta_{ij}. \quad (2.6)$$

The N values of $\mathbf{y}$ are confined to the first Brillouin zone which, for NaCl structure, is chosen such that the integers h_i are restricted by

$$-\tfrac{1}{2}<h_i/L\leqslant\tfrac{1}{2}, \quad (2.7a)$$

$$-\tfrac{3}{4}<\pm h_1/L\pm h_2/L\pm h_3/L\leqslant\tfrac{3}{4}. \quad (2.7b)$$

The secular determinant Eq. (2.4) now factorizes such that for each $\mathbf{y}$ there are $3n$ frequencies and normal coordinates $\omega(\mathbf{y},\gamma)$ and $Q(\mathbf{y},\gamma)$ ($\gamma=1, \cdots, 3n$). Similarly, the ion index K becomes the pair of indices l ($l=1, \cdots, N$) and k ($k=1, \cdots, n$), which designate a unit lattice cell and an ion within a cell respectively. $u_\alpha(K)$ and M_K are written as $u_\alpha(l,k)$ and M_k. The coordinate

transformation coefficients $e_\alpha(K;\, j)$ become[6]

$$e_\alpha(K;\, j)=e^{2\pi i\mathbf{y}\cdot\mathbf{x}(l,k)}e_\alpha(k;\, \mathbf{y},\gamma)\,, \tag{2.8}$$

where $\mathbf{x}(l,k)$ is the position of the kth ion in the lth lattice cell and the coefficients $e_\alpha(k;\, \mathbf{y},\gamma)$, called eigenvector components, are associated with the determination of the normal frequencies.

The inverse of the transformation Eq. (2.2) reads

$$u_\alpha(l,k)=\frac{1}{\sqrt{N}}\sum_{\mathbf{y}}^{N}\sum_{\gamma}^{3n} e^{2\pi i\mathbf{y}\cdot\mathbf{x}(l,k)}\frac{e_\alpha(k;\, \mathbf{y},\gamma)}{\sqrt{M_k}}Q(\mathbf{y},\gamma)\,. \tag{2.9}$$

For NaCl structure we may choose the eigenvectors as real and such that they transform as $\mathbf{y}$:

$$\mathbf{e}(k;\, -\mathbf{y},\, \gamma)=-\mathbf{e}(k;\, \mathbf{y},\gamma)\,. \tag{2.10}$$

The reality of Eq. (2.9), taken together with the convention Eq. (2.10), implies that

$$Q^*(\mathbf{y},\gamma)=-Q(-\mathbf{y},\, \gamma)\,. \tag{2.11}$$

It is convenient to introduce real normal coordinates $q_1(\mathbf{y},\gamma)$ and $q_2(\mathbf{y},\gamma)$ defined by

$$Q(\mathbf{y},\gamma)=(1/\sqrt{2})[q_1(\mathbf{y},\gamma)+iq_2(\mathbf{y},\gamma)]\,. \tag{2.12}$$

It follows that

$$q_1(-\mathbf{y},\, \gamma)=-q_1(\mathbf{y},\gamma)\,, \tag{2.13a}$$

$$q_2(-\mathbf{y},\, \gamma)=q_2(\mathbf{y},\gamma)\,. \tag{2.13b}$$

In expressing ion displacements in terms of the real normal coordinates, Eqs. (2.13) and (2.10) may be used. One restricts the summation over $\mathbf{y}$ to $\frac{1}{2}N$ points in reciprocal space that lie on one side of a plane passing through the origin of the Brillouin zone. Thus

$$\mathbf{u}(l,k)=\frac{\sqrt{2}}{\sqrt{N}}\sum_{\mathbf{y}}^{\frac{1}{2}N}\sum_{\gamma}^{3n}\frac{\mathbf{e}(k;\, \mathbf{y},\gamma)}{\sqrt{M_k}}[q_1(\mathbf{y},\gamma)\,\cos 2\pi\mathbf{y}\cdot\mathbf{x}(l,k) -q_2(\mathbf{y},\gamma)\,\sin 2\pi\mathbf{y}\cdot\mathbf{x}(l,k)]\,. \tag{2.14}$$

Similarly, the potential function becomes

$$\Phi_2=\tfrac{1}{2}\sum_{\mathbf{y}}^{\frac{1}{2}N}\sum_{\gamma}^{3n}\sum_{\lambda}^{2}\omega^2(\mathbf{y},\gamma)q_\lambda{}^2(\mathbf{y},\gamma)=\tfrac{1}{2}\sum_{j}^{3nN}\omega^2(j)q^2(j)\,, \tag{2.15}$$

where j is a collective index for $(\mathbf{y},\gamma,\lambda)$. We take Eq. (2.18) as our perfect crystal potential V_P. The quantities $\omega^2(\mathbf{y},\gamma)$ and $e_\alpha(k;\, \mathbf{y},\gamma)$ have been calculated by a number of workers[7] for several crystals of interest from various models of the quadratic coupling coefficients $\Phi_{\alpha\alpha'}(K,K')$. We consider the frequencies and eigenvectors as known quantities.

[6] The $\mathbf{e}(k;\, \mathbf{y},\gamma)$ are the eigenvectors of Ref. 2, Sec. 24; the eigenvectors of Sec. 38 differ by the phase factor $\exp[2\pi i\mathbf{y}\cdot\mathbf{x}(k)]$, where $\mathbf{x}(k)$ is the position of the kth ion in the zeroth cell.

[7] Some of the lattice vibration calculations are: (a) E. W. Kellermann, Phil. Trans. Roy. Soc. London **A238**, 513 (1940); (b) A. M. Karo and J. R. Hardy, Phys. Rev. **129**, 2074 (1963); (c) S. S. Jaswal (private communication).

Scalar Electron-Lattice Interaction Potential

In general, an electromagnetic interaction may be described by a vector potential and a scalar potential. The primary electron-phonon interaction occurs through the scalar potential since the motions of the electrons and ions are small compared to the velocity of light. We derive below a scalar electron-lattice interaction potential. The potential is resolved into a Fourier series whose maximum wavelength equals that of the phonon. We only keep this component to obtain the interactions.

Consider first the microscopic fields of a point-ion lattice undergoing harmonic vibrations. Following BH, Sec. 44, we use the microscopic Maxwell equation

$$\nabla\cdot\mathbf{E}^{\parallel}=4\pi\rho \tag{2.16}$$

and the equation of continuity

$$\nabla\cdot\mathbf{J}^{\parallel}=-\dot{\rho}\,. \tag{2.17}$$

Hence

$$\dot{\mathbf{E}}^{\parallel}=-4\pi\mathbf{J}^{\parallel}\,. \tag{2.18}$$

$\mathbf{E}^{\parallel}$ and $\mathbf{J}^{\parallel}$ are the longitudinal (lamellar, irrotational) parts of the microscopic electric field and current density, respectively. We have used the fact[8] that any vector $\mathbf{v}$ may be written as the sum of its longitudinal part $\mathbf{v}^{\parallel}$ and its transverse (solenoidal, rotational) part $\mathbf{v}^{\perp}$, where $\nabla\times\mathbf{v}^{\parallel}\equiv 0$ and $\nabla\cdot\mathbf{v}^{\perp}\equiv 0$. The microscopic current density may be expressed as follows[9]:

$$\mathbf{J}=\sum_l\sum_k e_k\delta[\mathbf{x}-\mathbf{x}(l,k)]\dot{\mathbf{u}}(l,k)\,, \tag{2.19}$$

where e_k is the ionic charge. From Eqs. (2.18) and (2.19) we obtain

$$\mathbf{E}^{\parallel}=-4\pi\sum_l\sum_k e_k\delta[\mathbf{x}-\mathbf{x}(l,k)]\mathbf{u}^{\parallel}(l,k)+\boldsymbol{\varepsilon}\,, \tag{2.20}$$

where $\mathbf{u}^{\parallel}(l,k)$ is the longitudinal part of $\mathbf{u}(l,k)$ and the constant of integration $\boldsymbol{\varepsilon}$ is the microscopic field for the ions fixed in their equilibrium positions, which we can delete from our calculations.

Using Eq. (2.9), Eq. (2.20) becomes

$$\mathbf{E}^{\parallel}=\sum_{\mathbf{y}}\sum_{\gamma}\left\{-\frac{4\pi}{\sqrt{N}}\sum_l\sum_k e_k\delta[\mathbf{x}-\mathbf{x}(l,k)]\frac{\mathbf{e}^{\parallel}(k;\, \mathbf{y},\gamma)}{\sqrt{M_k}} \times Q(\mathbf{y},\gamma)\,\exp\{2\pi i\mathbf{y}\cdot[\mathbf{x}(l,k)-\mathbf{x}]\}\right\}e^{2\pi i\mathbf{y}\cdot\mathbf{x}}\,. \tag{2.21}$$

$\mathbf{e}^{\parallel}(k;\, \mathbf{y},\gamma)$ is the component of $\mathbf{e}$ parallel to $\mathbf{y}$. The expression in large curly brackets is a periodic function of the lattice and therefore representable by a Fourier

[8] J. G. Coffin, *Vector Analysis* (John Wiley & Sons, Inc., New York, 1911), 2nd ed., p. 155.

[9] See Eq. (44.20) of Ref. 3. The small displacements $\mathbf{u}(l,k)$ have been omitted from the δ functions, which has the effect of centering each ion's current-density contribution at the ion's equilibrium position.

series:

$$\{\ \}=\sum_h \mathbf{E}^{\parallel}(h;\mathbf{y},\gamma)\exp[2\pi i\mathbf{w}(h)\cdot\mathbf{x}], \quad (2.22)$$

where the expansion wave vectors $\mathbf{w}(h)$ reflect the translational symmetry of the lattice; i.e., $\mathbf{w}(h)$ are the reciprocal-lattice vectors

$$\mathbf{w}(h)=h_1\mathbf{b}_1+h_2\mathbf{b}_2+h_3\mathbf{b}_3;\quad h_1,h_2,h_3=0,\pm1,\pm2,\cdots. \quad (2.23)$$

The Fourier coefficients are readily evaluated (BH, p. 215):

$$\begin{aligned}&\mathbf{E}^{\parallel}(h;\mathbf{y},\gamma)\\&=\frac{1}{v_a}\int_{\text{zero cell}}d\tau\left\{-\frac{4\pi}{\sqrt{N}}\sum_l\sum_k e_k\delta[\mathbf{x}-\mathbf{x}(l,k)]\right.\\&\quad\times\frac{\mathbf{e}^{\parallel}(k;\mathbf{y},\gamma)}{\sqrt{M_k}}Q(\mathbf{y},\gamma)\exp[2\pi i\mathbf{y}\cdot(\mathbf{x}(l,k)-\mathbf{x})\\&\quad\left.-2\pi i\mathbf{w}(h)\cdot\mathbf{x}]\right\}\\&=-\frac{4\pi}{v_a\sqrt{N}}\sum_k e_k\frac{\mathbf{e}^{\parallel}(k;\mathbf{y},\gamma)}{\sqrt{M_k}}Q(\mathbf{y},\gamma)\\&\quad\times\exp[-2\pi i\mathbf{w}(h)\cdot\mathbf{x}(k)]. \quad (2.24)\end{aligned}$$

Here v_a is the volume of a unit cell and is given by $2r_0^3$, where r_0 is the distance between nearest neighbors.

From Eqs. (2.21), (2.22), and (2.24) it follows that the microscopic field may be written

$$\begin{aligned}\mathbf{E}^{\parallel}&=-\frac{4\pi}{v_a\sqrt{N}}\sum_{\mathbf{y}}\sum_{\gamma}Q(\mathbf{y},\gamma)\sum_h\exp\{2\pi i[\mathbf{y}+\mathbf{w}(h)]\cdot\mathbf{x}\}\\&\quad\times\sum_k e_k\frac{\mathbf{e}^{\parallel}(k;\mathbf{y},\gamma)}{\sqrt{M_k}}\exp[-2\pi i\mathbf{w}(h)\cdot\mathbf{x}(k)]. \quad (2.25)\end{aligned}$$

For every $Q(\mathbf{y},\gamma)$ there is a macroscopic field associated with $h=0$ and some detailed structure within every cell when $\mathbf{w}(h)\neq0$. Our technique does not give the field within the cell since we consider the ions to be point charges. This ion can be displaced and polarized; hence, this does not correspond to the "point-ion model" developed by Gourary and Adrian. Furthermore, in most calculations of the wave functions one obtains the envelope wave functions and ignores the variations of the potential within the cells. Hence, one requires only the field corresponding to $h=0$. We therefore consider only this term and write (see also BH, p. 332)

$$\begin{aligned}\boldsymbol{\varepsilon}^{\parallel}&=-\frac{4\pi}{v_a\sqrt{N}}\sum_{\mathbf{y}}\sum_{\mathbf{x}}\sum_k e_k\frac{\mathbf{e}^{\parallel}(k;\mathbf{y},\gamma)}{\sqrt{M_k}}Q(\mathbf{y},\gamma)\\&\quad\times\exp(2\pi i\mathbf{y}\cdot\mathbf{x}). \quad (2.26)\end{aligned}$$

The complex normal coordinates may be replaced by the real normal coordinates by using Eq. (2.12), and the summation over $\mathbf{y}$ can be restricted to one-half the Brillouin zone by using the conditions imposed by Eqs. (2.10) and (2.13):

$$\begin{aligned}\boldsymbol{\varepsilon}^{\parallel}&=-\frac{4\pi\sqrt{2}}{v_a\sqrt{N}}\sum_{\mathbf{y}}\sum_{\gamma}\sum_{\lambda=1,2}\sum_k e_k\\&\quad\times\left[\left(\frac{\mathbf{y}}{|\mathbf{y}|}\right)\cdot\frac{\mathbf{e}(k;\mathbf{y},\gamma)}{\sqrt{M_k}}\right]\left(\frac{\mathbf{y}}{|\mathbf{y}|}\right)q_\lambda(\mathbf{y},\gamma), \quad (2.27)\\&\quad\times\cos2\pi\mathbf{y}\cdot\mathbf{x},\quad \lambda=1\\&\quad\times-\sin2\pi\mathbf{y}\cdot\mathbf{x},\quad \lambda=2\end{aligned}$$

where

$$\mathbf{e}^{\parallel}(k,\mathbf{y},\gamma)=[(\mathbf{y}/|\mathbf{y}|)\cdot\mathbf{e}(k;\mathbf{y},\gamma)](\mathbf{y}/|\mathbf{y}|). \quad (2.28)$$

We introduce the macroscopic scalar electric potential V, consistent with the Coulomb gauge, such that

$$-\nabla V=\boldsymbol{\varepsilon}^{\parallel}. \quad (2.29)$$

A solution for V may be readily found from inspection:

$$\begin{aligned}V&=\frac{2\sqrt{2}}{v_a\sqrt{N}}\sum_{\mathbf{y}}\sum_{\gamma}\sum_{\lambda=1,2}\sum_k e_k\\&\quad\times\left[\left(\frac{\mathbf{y}}{|\mathbf{y}|}\right)\cdot\frac{\mathbf{e}(k;\mathbf{y},\gamma)}{\sqrt{M_k}}\right]\frac{1}{|\mathbf{y}|}q_\lambda(\mathbf{y},\gamma) \quad (2.30)\\&\quad\times\sin2\pi\mathbf{y}\cdot\mathbf{x},\quad \lambda=1\\&\quad\times\cos2\pi\mathbf{y}\cdot\mathbf{x},\quad \lambda=2.\end{aligned}$$

The electron-lattice interaction potential is the electron's charge times V.

We can show that a similarity exists between this interaction potential and that of Fröhlich[5] (also see BH, Sec. 8, and Refs. 2a and 2b). Fröhlich has considered a phenomenological Hamiltonian written in terms of the lattice infrared polarization [e.g., Eq. (2.22) of Ref. 5]:

$$\begin{aligned}\mathcal{H}&=\mathcal{H}_{\text{electron}}+\mathcal{H}_{\text{lattice}}+\mathcal{H}_{\text{interaction}}\\&=\mathcal{H}_{\text{electron}}+\tfrac{1}{2}\gamma\int d^3r[(\dot{\mathbf{P}}_{\text{i.r.}}^{\parallel})^2+\omega^2(\mathbf{P}_{\text{i.r.}}^{\parallel})^2]\\&\quad-e\int d^3r\,\mathbf{D}\cdot\mathbf{P}_{\text{i.r.}}^{\parallel}, \quad (2.31)\end{aligned}$$

where the constant γ in Eq. (2.31) is given by

$$1/\gamma=(\omega^2/4\pi)(1/\epsilon_\infty-1/\epsilon).$$

ω is the frequency of the longitudinal optical modes in the long-wavelength limit; ϵ_∞ and ϵ are the high-frequency and static-dielectric constants, respectively. The interaction potential satisfies

$$-\text{grad}V=-4\pi\mathbf{P}_{\text{i.r.}}^{\parallel}. \quad (2.32)$$

This may be compared to the field term due to the $(\mathbf{y},\gamma)$ mode's contribution to the potential given by Eq. (2.29):

$$-\frac{4\pi}{v_a}\sum_k e_k\left[\frac{\mathbf{e}^{||}(k;\mathbf{y},\gamma)}{\sqrt{N}\sqrt{M_k}}Q(\mathbf{y},\gamma)e^{2\pi i\mathbf{y}\cdot\mathbf{x}}\right]. \quad (2.33)$$

When $\mathbf{x}$ has the value $\mathbf{x}(l,k)$, the term in square brackets is just the $(\mathbf{y},\gamma)$ mode's longitudinal displacement of the (l,k) ion from its equilibrium position. Thus, the quantity Eq. (2.33) appears as -4π times the longitudinal macroscopic polarization produced by a vibration mode. Although the interaction field of the potential Eq. (2.30) and the Fröhlich interaction field may both be viewed as polarization terms, the restrictions imposed by phenomenological considerations have been removed, i.e., a simple single-frequency lattice model has been avoided.

The rigid or point-ion model of the lattice employed in the derivation of the potential may be superseded by a more realistic ion model in a simple way. From the work of Szigeti[10] (see also BH, p. 112) we see that some allowance for the fact that the ions are extended polarizable charge distributions may be taken into account by assigning to the ions an effective charge of magnitude $s|e|$:

$$|e_k| = s|e|\,, \quad (2.34)$$

where $|e|$ is the magnitude of the electron charge and s is the Szigeti charge coefficient. These have been tabulated for a number of ionic crystals in the above-mentioned references. The use of the Szigeti charge coefficients is consistent with the lattice-vibration data used in the calculations (see Sec. V). These data have been computed on the basis of the Karo-Hardy[7b] deformation dipole model by Jaswal.[7c]

To simplify the notation, the real normal coordinates are denoted by the single index j replacing the $(\mathbf{y},\gamma,\lambda)$. The electron-lattice scalar potential energy takes the form

$$-eV = -e\sum_j f(j;\mathbf{r})q_j\,, \quad (2.35)$$

where the $f(j;\mathbf{r})$ are the functional coefficients of Eq. (2.30). $\mathbf{r}$ is the position of the electron.

III. EIGENSTATES OF SYSTEM

Here we are concerned with the problem of determining the shape of optical bands; hence the main interest is in the lattice-vibrational eigenstates. The Born-Oppenheimer technique is used to investigate these eigenstates as a function of electronic states. The procedure follows techniques outlined previously.[11]

The total system Hamiltonian is given by

$$\mathcal{H} = T_I + t + V_T\,, \quad (3.1)$$

where T_I and t are the kinetic-energy operators for the ions and the trapped electron (or electrons), respectively. The electronic Hamiltonian is defined as follows:

$$\mathcal{H}_e = t + V_T\,. \quad (3.2)$$

For each fixed ion configuration, and hence fixed set of generalized ion coordinates q_j (the set being denoted by $\mathbf{q}$), this Hamiltonian defines an electronic Schrodinger problem:

$$\mathcal{H}_e\varphi_n(\mathbf{q};\mathbf{r}) = \epsilon_n(\mathbf{q})\varphi_n(\mathbf{q};\mathbf{r})\,. \quad (3.3)$$

One can introduce *any set* of linearly independent $\mathbf{q}$, of which there are an infinite number. The eigenvalues and eigenfunctions depend on the particular frozen configuration $\mathbf{q}$. The total system eigenstates are approximated by

$$\Psi_{n,v}(\mathbf{q};\mathbf{r}) = \varphi_n(\mathbf{q};\mathbf{r})\chi_{n,v}(\mathbf{q})\,, \quad (3.4)$$

where v denotes additional quantum numbers. Substitution into the eigenvalue problem

$$\mathcal{H}\Psi_{n,v} = E_{n,v}\Psi_{n,v} \quad (3.5)$$

yields

$$\varphi_n[T_I+\epsilon_n(\mathbf{q})]\chi_{n,v} + \mathfrak{L}(\varphi_n\chi_{n,v}) = \varphi_n E_{n,v}\chi_{n,v}\,. \quad (3.6)$$

$\mathfrak{L}(\varphi_n\chi_{n,v})$ is the nonadiabatic term. It is conventional to delete this term; thus,

$$[T_I+\epsilon_n(\mathbf{q})]\chi_{n,v}(\mathbf{q}) = E_{n,v}\chi_{n,v}(\mathbf{q})\,. \quad (3.7)$$

Two interesting features of Eq. (3.7) are: (i) The electronic eigenvalue becomes the potential function of the lattice Schrödinger equation; (ii) the lattice eigenvalue is taken to be the total energy of the system.

The potential $\epsilon_n(\mathbf{q})$ can be expanded:

$$\epsilon_n(\mathbf{q}) = \epsilon_n(0) + \sum_j \epsilon_n(j)q_j + \tfrac{1}{2}\sum_{j,j'}\epsilon_n(j,j')q_jq_{j'} + \cdots\,. \quad (3.8)$$

For any given set of $\mathbf{q}$'s we may always write

$$V_T = g_0(\mathbf{r}) + \sum_j g_1(j;\mathbf{r})q_j + \tfrac{1}{2}\sum_j \omega^2(j)q_j^2 + \tfrac{1}{2}\sum_{j,j'} g_2(j,j';\mathbf{r})q_jq_{j'} + \cdots\,, \quad (3.9)$$

where the ω's are not a true angular frequencies since g_1 and g_2 do not equal zero. The only problem ignored here is that there could be fewer degrees of freedom in the actual crystal. In the case of an F center, the crystal has three degrees of freedom missing because of the ionic vacancy.

The electronic energy is

$$\epsilon_n(\mathbf{q}) = \int d^3r\ \varphi_n^*(\mathbf{q};\mathbf{r})\mathcal{H}_e\varphi_n(\mathbf{q};\mathbf{r})\,. \quad (3.10)$$

Furthermore,

$$\epsilon_n(0) \equiv \epsilon_n(\mathbf{q}=0) = \int d^3r\ \varphi_n^*(\mathbf{q}=0;\mathbf{r})[t+g_0(\mathbf{r})]\varphi_n(\mathbf{q}=0;\mathbf{r}) \quad (3.11)$$

[10] B. Szigeti, Trans. Faraday Soc. **45**, 155 (1949); Proc. Roy. Soc. (London) **A204**, 51 (1950).
[11] J. J. Markham, Rev. Mod. Phys. **31**, 956 (1959).

and

$$\epsilon_n(j)=\int d^3r\ \varphi_n^*(\mathbf{q}=0;\mathbf{r})\frac{\partial V_T}{\partial q_j}\bigg|_{q=0}\varphi_n(\mathbf{q}=0;\mathbf{r})$$

$$=\int d^3r\ |\varphi_n|^2 g_1(j;\mathbf{r}), \tag{3.12}$$

where the Feynman theorem (BH, p. 189) has been used. The linear lattice-potential coefficients are determined by the linear total-potential coefficients of Eq. (3.9) and the electronic eigenfunctions.

If the true normal coordinates $q_n(j)$ had been introduced, the lattice Hamiltonian would have the form

$$\mathfrak{IC}_n(L)=T_I+\bar{\epsilon}_n(0)+\tfrac{1}{2}\sum_j \omega_n^2(j)q_n^2(j). \tag{3.13}$$

If $\epsilon_n(j,j')=0$ for $j'\neq j$, one may relate (3.13) to (3.8) as follows:

$$q_n(j)=q_j-\Delta q_n(j), \tag{3.14}$$

$$\omega_n^2(j)=\omega^2(j)+t_n(j,j), \tag{3.15}$$

where

$$\Delta q_n(j)=-\frac{\epsilon_n(j)}{\omega_n^2(j)}=-\frac{1}{\omega_n^2(j)}\int d^3r\ |\varphi_n|^2 g_1(j;\mathbf{r}). \tag{3.16}$$

(See Ref. 11, p. 959, for details.) In view of (3.13), the lattice functions have the form

$$\chi_{n,v}=\prod_j \chi_n[v_j;\omega_n^2(j),q_n(j)]$$

$$\cong\prod_j \chi_n[v_j;\omega^2(j)+t_n(j,j),\ q_j-\Delta q_n(j)]. \tag{3.17}$$

We stress that the simple product form applies only to the q_n's and not to our arbitrary set introduced in Eq. (3.3). The true modes of a crystal with an imperfection are not the perfect lattice modes.

Omission of the $\epsilon_n(j,j')$ terms for $j'\neq j$ may be a rather crude approximation, as it can be shown that this neglects the eigenvector effect (a change of the eigenvectors from those of the perfect lattice, particularly for ions in the vicinity of the defect) discussed by Casselman and Markham[12a] and by McCombie, Matthew, and Murray.[12b]

IV. METHOD OF LINE-SHAPE ANALYSIS

We are *primarily* concerned with defect-center optical-spectra band shapes in which there is detailed attendant phonon structure. A direct method of line-shape analysis is described that is suitable for this calculation. The fundamental details of the theory of optical transitions is left to the references (e.g., Dexter[13] or Markham[4]).

[12] (a) T. N. Casselman and J. J. Markham, J. Phys. Chem. Solids **24**, 669 (1963); (b) C. W. McCombie, J. A. D. Matthew, and A. M. Murray, J. Appl. Phys. Suppl. **33**, 359 (1962).

[13] D. L. Dexter, Solid State Phys. **6**, 353 (1958).

In the Condon and dipole approximations, the optical transition rate associated with light of *angular* frequency ν and a definite imperfection electron transition from a state g (ground) to a state u (upper) is proportional to

$$\alpha(\nu)=Kf_{ug}[\mathrm{Av}_T\sum_{v'}|\{\chi_{u,v'}|\chi_{g,v}\}|]^2$$
$$\times\delta[(E_{u,v'}-E_{g,v})-\hbar\nu], \tag{4.1}$$

where δ is the Dirac δ function, f_{ug} is the transition oscillator strength

$$f_{ug}=\frac{4\pi}{3}\frac{m}{h}\nu\left[\int d^3r\ \varphi_u^*\mathbf{r}\varphi_g\right]^2, \tag{4.2}$$

and K involves such factors as an "effective field ratio" and the concentration of imperfections. $E_{u,v'}$ and $E_{g,v}$ are the upper and ground-state system energies (lattice-state eigenvalues), respectively; $E_{u,v'}-E_{g,v}$ includes the electronic-state transition energy and the change in the vibrational energy of the lattice. $\sum_{v'}$ denotes a summation over all possible final lattice states, while Av_T denotes a thermal average of the initial states.

Using the closure relationship

$$\sum_{v'}|\chi_{u,v'}\}\{\chi_{u,v'}|=1, \tag{4.3}$$

it follows that

$$\mathrm{Av}_T\sum_{v'}|\{\chi_{u,v'}|\chi_{g,v}\}|^2$$
$$=\mathrm{Av}_T\sum_{v'}\{\chi_{g,v}|\chi_{u,v'}\}\{\chi_{u,v'}|\chi_{g,v}\}$$
$$=\mathrm{Av}_T\{\chi_{g,v}|\chi_{g,v}\}=1. \tag{4.4}$$

Therefore, if we neglect the frequency dependence of Kf_{ug}, this result means that the quantity in square brackets of Eq. (4.1) is a normalized absorption line-shape function. The overlap matrix element $M_{ug}{}^j\times(v_j',v_j)$ is defined as

$$M_{ug}{}^j(v_j',v_j)=\{\chi_u[v_j';\omega_u^2(j),\ q_j-\Delta q_u(j)]|$$
$$\times\chi_g[v_j;\omega_g^2(j),\ q_j-\Delta q_g(j)]\}. \tag{4.5}$$

The normalized line shape is described in terms of a distribution of quantities $\mathrm{Av}_T\prod_j|M_{ug}{}^j(v_j',v_j)|^2$.

We make the assumption that the change in the normal coordinates is the dominant effect in coupling different vibrational levels and we neglect *the change in the lattice frequencies* accompanying an electronic transition; hence $\omega_g(j)=\omega_u(j)=\omega_j$. To systematize the calculations, the per-mode Huang-Rhys factor is defined

$$S_j=[q_u(j)-q_g(j)]^2\omega_j/2\hbar$$
$$=[\Delta q_u(j)-\Delta q_g(j)]^2\omega_j/2\hbar. \tag{4.6}$$

Using Eq. (3.16), S_j becomes

$$S_j=\frac{[\epsilon_u(j)-\epsilon_g(j)]^2}{2\hbar\omega_j{}^3}$$
$$=\frac{1}{2\hbar\omega_j{}^3}\left[\int d^3r\; g_1(j;\mathbf{r})(|\varphi_u|^2-|\varphi_g|^2)\right]^2. \quad (4.7)$$

It can be shown[14] that, in the approximation employed, $M_{ug}{}^j(v_j',v_j)$ is given by

$$M_{ug}{}^j(v_j',v_j)=[(v_j)!/(v_j')!]^{1/2}\times e^{-S_j/2}(S_j)^{(v_j'-v_j)/2}L_{v_j}{}^{(v_j'-v_j)}(S_j), \quad (4.8)$$

where $L_b{}^a(x)$ is an associated Laguerre polynomial.

In order to simplify the discussion to follow, we consider only the limiting case of extremely low temperatures, i.e., $v_j=0$. For this case, the matrix element Eq. (4.8) has the simpler form[15]

$$M_{ug}{}^j(v_j',0)=[S_j{}^{v_j'}e^{-S_j}/(v_j')!]^{1/2}. \quad (4.9)$$

The transition which leaves all the vibration modes unexcited (i.e., all $v_j'=0$) constitutes the zero-phonon line, which has zero width in our approximate model. The contribution of this line is

$$I_0(\hbar\nu)=\prod_j |M_{ug}{}^j(0,0)|^2\delta[\hbar(\nu-\nu_{ug})]$$
$$=e^{-S}\delta[\hbar(\nu-\nu_{ug})], \quad (4.10)$$

where ν_{ug} is the angular frequency of the zero-phonon line and

$$S=\sum_j S_j. \quad (4.11)$$

Thus, e^{-S} is the ratio of the zero-phonon line intensity to the integrated intensity of the entire spectrum, or the zero-phonon relative transition probability. S is the generalized Huang-Rhys factor or "S factor" used by many authors.[4]

The transition event in which a single phonon is created in the jth mode, all other modes remaining unexcited, contributes to the spectrum according to

$$i_1(\hbar\nu)$$
$$=|M_{ug}{}^j(1,0)|^2\prod_{j'\neq j}|M_{ug}{}^{j'}(0,0)|^2\delta[\hbar\nu-\hbar(\nu_{ug}\pm\omega_j)]$$
$$=e^{-S}S_j\delta[\hbar\nu-\hbar(\nu_{ug}\pm\omega_j)], \quad (4.12)$$

where the plus sign corresponds to absorption and the minus to emission. Therefore, the contribution of one-phonon processes to the spectrum in the energy range between $\hbar(\nu_{ug}\pm\omega)$ and $\hbar[\nu_{ug}\pm(\omega+\Delta\omega)]$ is

$$I_1[\hbar(\nu_{ug}\pm\omega)]\hbar\Delta\omega$$
$$=\int_{\hbar\omega}^{\hbar(\omega+\Delta\omega)}\hbar d\nu\; i_1(\hbar\nu)=e^{-S}\sum_{\hbar\omega_j=\hbar\omega}^{\hbar(\omega+\Delta\omega)}S_j. \quad (4.13)$$

We define the distribution $s_1(\hbar\omega)$ as follows:

$$s_1(\hbar\omega)=\frac{1}{\hbar\Delta\omega}\sum_{\hbar\omega_j=\hbar\omega}^{\hbar(\omega+\Delta\omega)}S_j. \quad (4.14)$$

Hence, the one-phonon spectrum intensity distribution is

$$I_1(\hbar\nu-\hbar\nu_{ug}=\pm\hbar\omega)=e^{-S}s_1(\hbar\omega). \quad (4.15)$$

The fraction of the integrated intensity due to one-phonon processes is

$$\int_{-\infty}^{\infty}dE\; I_1(E)=\int_{-\infty}^{\infty}dE\; e^{-S}s_1(E)=e^{-S}S. \quad (4.15')$$

The relative probability of a transition creating just two phonons in the jth and j'th modes is

$$|M_{ug}{}^j(1,0)|^2|M_{ug}{}^{j'}(1,0)|^2\prod_{j''\neq j,j'}|M_{ug}{}^{j''}(0,0)|^2$$
$$=S_jS_j\cdot e^{-S}\quad(j'\neq j) \quad (4.16a)$$

or

$$|M_{ug}{}^j(2,0)|^2\prod_{j''\neq j}|M_{ug}{}^{j''}(0,0)|^2$$
$$=\frac{1}{2!}S_j{}^2e^{-S}\quad(j'=j). \quad (4.16b)$$

Therefore, the two-phonon spectrum intensity distribution may be expressed as

$$I_2(\hbar\nu-\hbar\nu_{ug}=\pm\hbar\omega)=e^{-S}s_2(\hbar\omega); \quad (4.17)$$

the two-phonon distribution $s_2(\hbar\omega)$ is defined by

$$s_2(\hbar\omega)=\frac{1}{\hbar\Delta\omega}[(1/2!)\sum_{\substack{j_1,j_2\\ \hbar\omega}}^{\hbar(\omega+\Delta\omega)}S_{j_1}S_{j_2}], \quad (4.18)$$

where $\hbar(\omega_{j_1}+\omega_{j_2})=\hbar\omega$. The $(1/2)!$ correctly weights the case of two phonons being created in the same mode, as well as taking into account that if the two different modes j and j' satisfy the energy conditions, then this term is counted 2! times by the sum. $s_2(E)$ may be expressed as a convolution of $s_1(E)$ as follows:

$$s_2(E)=(1/2!)\int_{-\infty}^{\infty}dE'\; s_1(E')s_1(E-E'). \quad (4.19)$$

It follows from Eqs. (4.15'), (4.17), and (4.19) that the fraction of the integrated spectrum arising from two-

[14] (a) T. H. Keil, Phys. Rev. **140**, A601 (1965); (b) J. T. Ritter, Ph.D. thesis, Illinois Institute of Technology, 1967 (unpublished).

[15] Equation (4.9) was first obtained by Pekar, based on the assumption that $\Delta q_n(j)\to 0$ and the number of modes are very large. Reference 11 gives a general proof for the case where the phonon frequencies are not effected by the electronic transition and calls the resulting band shape "Pekarian." However, $|M_{ug}{}^j(v_j,0)|^2$ actually gives the Poisson distribution [see Eq. (4.21)].

phonon processes is

$$\int_{-\infty}^{\infty} dE I_2(E) = e^{-S}\int_{-\infty}^{\infty} dE s_2(E) = e^{-S}S^2/2!. \quad (4.17')$$

We may generalize to the case of the n-phonon distribution $s_n(E)$:

$$s_n(E) = \frac{1}{\Delta E}[(1/n!)\sum_{\substack{j_1,j_2\cdots j_n \\ E}}^{E+\Delta E} S_{j_1}S_{j_2}\cdots S_{j_n}], \quad (4.20a)$$

where $\hbar(\omega_{j_1}+\cdots+\omega_{j_n})=E$. If one term of Eq. (4.20) involves n different modes, then the factor $(1/n!)$ accounts for the $n!$ rearrangements of this term. If a contribution involves the creation of L phonons in the lth mode, L' phonons in the l'th mode, etc., then the $(1/n!)$ accounts for the repetitions of this term and properly weights it by $(1/L!)$, $(1/L'!)$, etc., as required by Eq. (4.9). The number of modes need not be large nor all S_j be small for this relationship to hold; it holds even if one employs a single mode in the calculations. The $s_n(E)$ may be expressed in terms of $s_1(E)$ as follows:

$$s_n(E) = \frac{1}{n!}\int_{-\infty}^{\infty} dE' \int_{-\infty}^{\infty} dE'' \cdots \int_{-\infty}^{\infty} dE^{n-1} \times s_1(E')s_1(E'')\cdots s_1[E-(E'+E''+\cdots+E^{n-1})], \quad (4.20b)$$

$$= \frac{1}{n}\int_{-\infty}^{\infty} dE'\, s_1(E')s_{n-1}(E-E'). \quad (4.20c)$$

Furthermore, the fraction of the spectrum's integrated intensity due to n-phonon processes is

$$P(n) = e^{-S}\int_{-\infty}^{\infty} dE\, s_n(E) = e^{-S}S^n/n!. \quad (4.21)$$

It is interesting to note that the discrete-phonon spectrum distribution having the largest fractional contribution to the integrated intensity occurs for an integer $n \approx (S-\frac{1}{2})$.

The total spectrum-distribution function is the sum of the distribution terms we have just considered; thus

$$I(\hbar\nu - \hbar\nu_{ug} = \pm E) = e^{-S}[\delta(\hbar\nu)+s_1(E)+\cdots+s_n(E)+\cdots]. \quad (4.22)$$

Since the integration of the nth term yields $S^n/n!$, which is the nth term in the series expansion of $\exp(S)$, it follows that Eq. (4.22) is a normalized line-shape function as expected.

In order to demonstrate the nature of the terms of Eq. (4.22), we shall consider the assumption that $s_1(E)$ is a Gaussian distribution centered about $\hbar\omega_e$ and of standard deviation σ:

$$s_1(E) = S[1/(2\pi)^{1/2}\sigma]\exp[-(E-\hbar\omega_e)^2/2\sigma^2]. \quad (4.23)$$

$s_n(E)$ is given by

$$s_n(E) = (S^n/n!)[1/(2\pi n)^{1/2}\sigma] \times \exp[-(E-n\hbar\omega_e)^2/2n\sigma^2]. \quad (4.24)$$

Thus s_n peaks at $n\hbar\omega_e$ and the standard deviation is $(\sqrt{n})\sigma$. If the interacting vibrational modes are envisioned as having a single effective frequency ω_e (as in either a single local mode or configurational coordinate model,[11] or the Fröhlich longitudinal optical modes model[2b]), then Eq. (4.22) is a series of δ functions $\hbar\omega_e$ apart and weighted according to a Poisson distribution. The broad F-center band is often described by a single effective frequency. We feel that the smoothness of the F band arises from phonon dispersion.

Equation (4.22) represents a possible method of calculating a spectrum line shape when the sum coverges rapidly. This means that S must be small in order for this to be a practical approach. This is the situation when a strong zero-phonon line and detailed discrete-phonon structure occurs. In lieu of this, we quote a result of the methods of moments[11] suitable for broad-band calculations. The important quantity is the square deviation m^2, defined by

$$m^2 = M_2/M_0 - (M_1/M_0)^2, \quad (4.25)$$

where M_n is the nth moment of the band. m^2 is given by

$$m^2 = \sum_j \hbar^2\omega_j^2 S_j \coth(\hbar\omega_j/2kT), \quad (4.26)$$

where T is the temperature. If the band shape is Gaussian or Poissonian with large S, then the full width at half-height $H(T)$ is given by

$$H^2(T) = (8\ln 2)m^2 = (8\ln 2)\sum_j \hbar^2\omega_j^2 S_j \coth(\hbar\omega_j/2kT). \quad (4.27)$$

We see that S_j also enters into broad-band calculations. S enters the calculation only in special situations where one can take averages over sums such as those appearing in Eq. (4.27). If a broad band is described by a single effective frequency ω_e, then

$$H^2(T) = (8\ln 2)\hbar^2\omega_e^2 S \coth(\hbar\omega_e/2kT) \quad \text{(special case)}. \quad (4.27')$$

V. CALCULATIONS

This section reports calculations on: (i) the F-center half-width in NaCl and KCl [16]; (ii) the one-phonon line shapes in LiF, NaCl, and KCl.[17] Both types of calcula-

[16] These calculations were reported previously [see Phys. Letters **25A**, 675 (1967)] and are included here for completeness.

[17] The KCl calculations have been partially reported previously [see Phys. Letters **24A**, 524 (1967)].

tion are based on the expression for S_j given by Eq. (4.7). In this equation the $g_1(j;\mathbf{r})$, which are the general linear coefficients of the system's potential, are taken to be $-ef(j;\mathbf{r})$, where the $f(j;\mathbf{r})$ are the scalar potential coefficients derived in Sec. II [see Eqs. (2.30) and (2.35)] and $-e$ is the electron charge. Since $(|\varphi_u|^2-|\varphi_g|^2)$ has even parity,

$$\int d^3r(|\varphi_u|^2-|\varphi_g|^2)\sin 2\pi\mathbf{y}\cdot\mathbf{r}=0,$$

we need evaluate only

$$I(\mathbf{y})=\int d^3r(|\varphi_u|^2-|\varphi_g|^2)\cos 2\pi\mathbf{y}\cdot\mathbf{r}. \quad (5.1)$$

S_j becomes

$$S_j=\frac{1}{2\hbar\omega_j}\left[\frac{e2\sqrt{2}}{v_a\sqrt{N}}\sum_k e_k\left(\frac{\mathbf{y}_j}{|\mathbf{y}_j|^2}\right)\cdot\frac{\mathbf{e}(k;j)}{\sqrt{M_k}}\right]^2 I^2(\mathbf{y}_j), \quad (5.2)$$

where the j's are selected so that $\lambda=2$. Perfect crystal vibration data (eigenvectors and frequencies) were used in all computations. These were calculated and supplied to us by Jaswal,[7c] who used the deformation dipole model developed by Karo and Hardy.[7b] Some computations were also made for comparison, using Kellermann[7a] rigid-ion-model data.[7c]

Half-Width of the *F* Band

If a broad-band center "sees" a single-phonon frequency ω_e, then Eq. (4.27′) applies and

$$\operatorname{arccoth}[H^2(T)/H^2(0)]$$

plotted against $\hbar/2kT$ is a straight line through the origin with ω_e as its slope. Such a plot with alkali-halide F-center data does form a straight line within the experimental error, and this defines an effective frequency for the center.[4] However, for some alkali halides the line does not extrapolate to the origin. For these cases[4,18] one plots

$$X(T,C)\equiv\operatorname{arccoth}[(H^2(T)-C)/(H^2(0)-C)]$$

against $\hbar/2kT$, where C is a constant chosen so that the straight lines extrapolate to the origin. We shall return to the question of the meaning of C.

The half-width calculations reported here assume that many-phonon frequencies are involved and Eq. (4.27) applies. For each case considered, the S_j were computed for a representative sampling of 6000 modes corresponding to a "Kellermann[7a] mesh" of 1000 wave-vector points $\mathbf{y}$ uniformly distributed in the Brillouin zone. By using NaCl symmetry, one need specifically consider only 48 points in 1/48 of the zone (see Kellermann for details). The wave functions used to compute the integral $I(\mathbf{y})$ were taken from the work of Fowler[19a] and of Gilbert.[19b] Their wave functions are "1s-like" ground-state functions $\varphi_g\sim(1+\alpha r)e^{-\alpha r}$ and $2p_z$ upper-state functions $\varphi_u\sim re^{-\beta r}\cos\theta$, where the α and β were determined from a self-consistent variational calculation. In these calculations φ_u were taken to be of a spherically symmetric form. $I(\mathbf{y})$ then depends only on the magnitude of $\mathbf{y}$ and can be analytically evaluated.

$X(T,C)$ plots were made with calculated $H(T)$ data. These plots are straight lines within the rounding-off errors (about 1%), and the slopes define the calculated effective lattice frequencies. However, C cannot be determined with much precision. Values of S were computed from Eq. (4.27′) with $T=0$. Calculated results are compared with experimental results in Table I.

A value of C determined from these calculations is nonzero because $H(T)$ is computed from a distribution of frequencies. Thus the calculations are fitted to a phe-

TABLE I. Calculations and experimental data for the F-center absorption and emission spectra in NaCl and KCl.

		Calculated data: Gilbert's wave functions	Calculated data: Fowler's wave functions	Experimental data[a]
	$\alpha(A^{-1})$	1.067	1.057	
	$\beta(A^{-1})$	0.821	0.782	
NaCl	$H(0)$ (eV)	0.250	0.192	0.255
Absorption	$\omega_e(10^{13}\ \mathrm{sec}^{-1})$	3.10	3.13	2.76
Data	C (eV^2)	0.004	0.005	−0.01[b]
	S	27	15.6	35.3[c]
	$\alpha(A^{-1})$	0.606	0.822	
	$\beta(A^{-1})$	0.078	0.189	
NaCl	$H(0)$ (eV)	0.404	0.485	0.337
Emission	$\omega_e(10^{13}\ \mathrm{sec}^{-1})$	4.20	3.91	3.71
Data	C(eV^2)	0.008	0.020	?
	S	38.4	63.9	34.3[c]
	$\alpha(A^{-1})$	0.995		
	$\beta(A^{-1})$	0.722		
KCl	$H(0)$ (eV)	0.173		0.163
Absorption	$\omega_e(10^{13}\ \mathrm{sec}^{-1})$	2.59		1.86
Data	C(eV^2)	0.0015		0.00[b]
	S	18.5		31.9[c]
	$\alpha(A^{-1})$[d]	0.462		
KCl	$\beta(A^{-1})$[d]	0.101		
Emission[d]	$H(0)$(eV)	0.294		0.261
Data	$\omega_e(10^{13}\ \mathrm{sec}^{-1})$	3.61		2.86
	C(eV^2)	0.005		?
	S	27.5		34.7[c]

[a] W. Gebhardt and H. Kuhnert, Phys. Letters **11**, 15 (1964).
[b] From Ref. 18.
[c] Recalculated from Ref. a, above. Some other values of S experimental are: for NaCl, 40 [see J. Markham and J. Konitzer, J. Chem. Phys. **34**, 1936 (1961)] and for KCl, 28.4 [see J. Konitzer and J. Markham, J. Chem. Phys. **32**, 843 (1960)].
[d] The values used in KCl emission are obtained by Gilbert in his thesis (case V_2). The published values have been corrected. The new values would give better agreement with experiment, but we have not repeated the calculations.

[18] J. J. Markham and J. D. Konitzer, J. Chem. Phys. **34**, 1936 (1961).

[19] (a) W. B. Fowler, Phys. Rev. **135**, A1725 (1964); (b) R. L. Gilbert, Ph.D. thesis, Illinois Institute of Technology, 1967 (unpublished).

nomenological single-frequency model in which the half-width obeys[11,18]

$$H^2(T)=C+D\coth(\hbar\omega_e/2kT), \qquad (5.3)$$

where C and D are constants (see Ref. 11, which discusses the possibility of C arising from an oscillator-strength dependence on the lattice normal coordinates). Figure 2 shows plots of $\operatorname{arccoth}[H^2(T)/H^2(0)]$ against $\hbar\omega_e/2kT$ for various ratios of C/D. (We use values of C that are larger than realistic in order to demonstrate the situation.) The appropriate C in an $X(T,C)$ plot produces the central straight line. There is a basic failure of these calculations to predict the proper sign of C (see the NaCl results in Table I). This failure may be because the calculations have neglected the dependence of the F-center wave functions and forms of the lattice vibrations upon temperature, or perhaps C is not primarily determined by phonon dispersion.

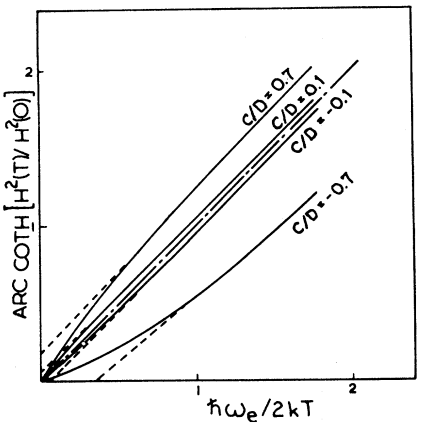

FIG. 2. Illustration of $X(T,C)$ plot when $H(T)$ is given by Eq. (3.5). Note that Fig. 8 of Ref. 11 was mislabeled.

The marked difference between effective frequencies for absorption and emission arises from the dependence of the electron-phonon interaction on the electron wave functions. Figure 3 shows $I(|\mathbf{y}|)$ calculated from Fowler's[19a] NaCl F-center absorption and emission wave functions. [Note that $I^2(|\mathbf{y}|)$ is actually required.] Since the emission wave functions are much more diffuse than those of absorption, longer-wavelength (smaller $|\mathbf{y}|$) phonons are more important in the emission band broadening. It is the relatively large contributions of the long-wavelength optic modes to the emission band that accounts for its effective frequency being substantially higher than that of the absorption band.

One-Phonon Line Shapes

A defect center whose spectrum shows detailed attendant phonon structure and a prominant zero-phonon line (relative intensity $=e^{-S}$) has a small S factor and the line-shape representation of Eq. (4.22) converges

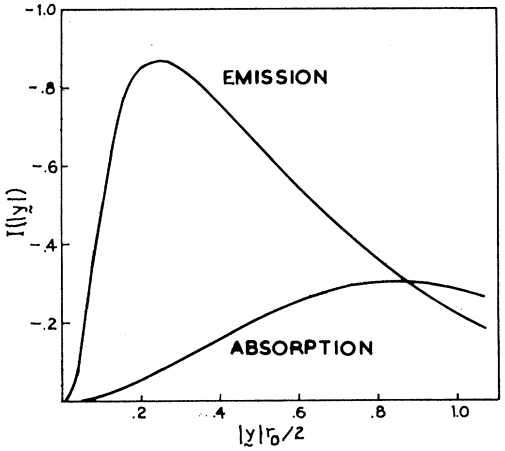

FIG. 3. $I(|\mathbf{y}|)$ as a function of reduced wave vector based on Fowler's (16a) NaCl wave functions.

rapidly. The calculations reported here are limited to the one-phonon distribution term since the S_j required could not be estimated with sufficient accuracy to warrant further consideration. However, the one-phonon region of a spectrum has the sharpest resolved structure and hence it can be compared to calculated phonon structure with the least ambiguity.

S_j of Eq. (5.2) is now written in the form

$$S_j=L_jF_j, \qquad (5.4)$$

where the factor L_j is defined by

$$L_j=\frac{1}{\omega_j^3}\left|\sum_k \frac{e_k}{e}\left(\frac{\mathbf{y}_j}{|\mathbf{y}_j|^2}\right)\cdot\frac{\mathbf{e}(k;j)}{\sqrt{M_k}}\right|^2. \qquad (5.5)$$

L_j is called the per-mode lattice factor and depends only on the lattice vibration data. F_j is given by

$$F_j=(4e^4/v_a{}^2N)I^2(\mathbf{y}_j). \qquad (5.6)$$

The wave functions are not known for those centers in alkali halides whose optical bands show discrete-phonon structure. Therefore, it is impossible to calculate F_j, and hence S_j. Correspondingly, we have made the assumption that a distribution formed from the L_j contains the essential features of the one-phonon distribution factor $s_1(\hbar\omega)$. This is equivalent to the assumption that $I(\mathbf{y}_j)$ is a constant independent of the mode j. Some feeling for the error that this introduces can be found from the F-center calculations above. It is clear from Eq. (5.1) that $F_j\to 0$ as $|\mathbf{y}_j|\to 0$ (see Fig. 3). Hence, our approach here greatly overestimates the long-wavelength modes.

For KCl, NaCl, and LiF crystals the L_j have been computed for the 6000 representative modes associated with the "Kellermann mesh" as for the F-center calculations. These L_j are grouped according to their frequency to form lattice-factor distributions. Comparisons are made between these distributions and phonon-

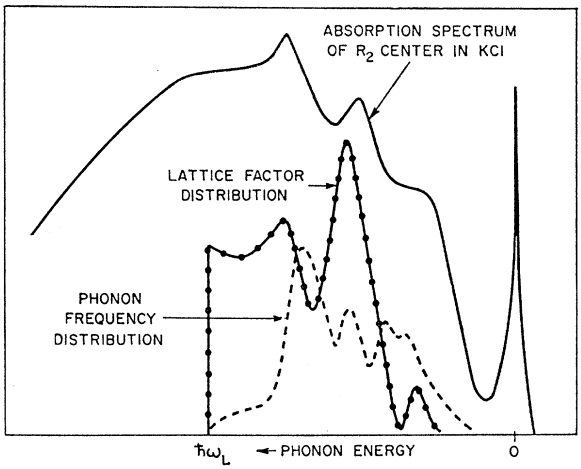

FIG. 4. Absorption spectrum of the KCl R_2 center [from Ref. 1(b)] compared to the lattice-factor distribution and density of vibration states. ($\hbar\omega_L=0.026$ eV).

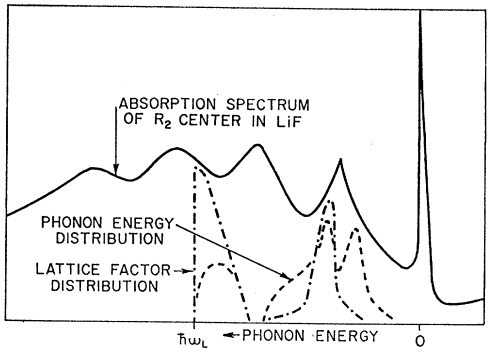

FIG. 6. Absorption spectrum of the LiF R_2 center [from Ref. 1(b)] compared to the lattice-factor distribution and density of vibration states ($\hbar\omega_L=0.0825$ eV). Note that peaks in the spectrum do *not* correspond to the gap between the vibration branches.

structured spectra of various F-aggregate centers by placing the origin of a lattice-factor distribution at the zero-phonon line of an experimental spectrum. Figures 4–6 show predicted line shapes from one-phonon contributions and the experimental absorption spectra of the R_2 centers in KCl, NaCl, and LiF, respectively, obtained from Ref. 1b. The calculated distributions of phonon states of the host crystals are also shown for comparison purposes. The observed line shapes contain, of course, multiphonon structure and they continue well past the photon-energy limit ($\hbar\nu_{u0}+\hbar\omega_L$) associated with one-phonon processes, where ω_L is the maximum angular frequency of the lattice phonons. The abrupt drop in the calculated one-phonon line shape at the phonon energy $\hbar\omega_L$ occurs because the factor F_j was neglected. If F_j were taken into account, the one-phonon line-shape distribution would go smoothly to zero as the phonon energy $\hbar\omega_L$ is approached. Thus the lattice-factor distribution's prediction of a feature in the spectrum at this point arises from an oversimplification of the calculations and is not a failure of the theory. Figures 7–9 show further comparisons between lattice-factor distributions of KCl, LiF, and NaCl crystals and the experimental spectra of the R' center (KCl) and M' center (LiF and NaCl). The experimental spectra have been redrawn from Fitchen, Fetterman, and Pierce[1b] (KCl and LiF) and Pierce[1c] (NaCl).

A NaCl lattice-factor distribution has also been computed from rigid-ion-model (Kellermann) vibration data. Figure 10 shows the NaCl R_2 center spectrum [from Ref. 1(b)] compared to one-phonon calculations based on both rigid-ion model and deformation dipole-model vibration data. In contradistinction to the results of the deformation dipole-model calculations, the rigid-ion-model calculations show poor agreement with experiment as to the positions of major features in the attendant phonon structure. This indicates that the deformation dipole model is a more realistic representation of the lattice vibrations than the older rigid-ion model.

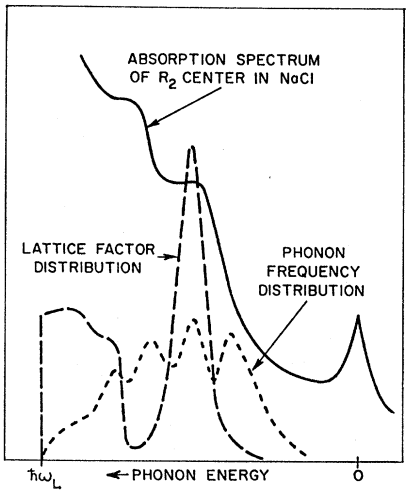

FIG. 5. Absorption spectrum of the NaCl R_2 center [from Ref. 1(b)] compared to the lattice-factor distribution and density of vibration states. ($\hbar\omega_L=0.0319$ eV).

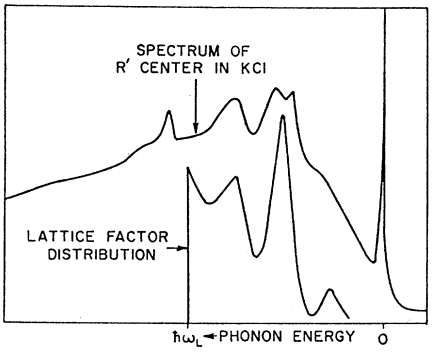

FIG. 7. Absorption spectrum of the KCl R' center [from Ref. 1(d)] compared to the lattice-factor distribution.

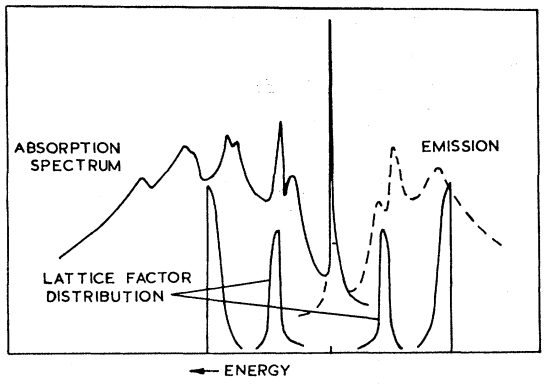

FIG. 8. Absorption and emission spectrum of the LiF M' center [from Ref. 1(d)] compared to the lattice-factor distribution.

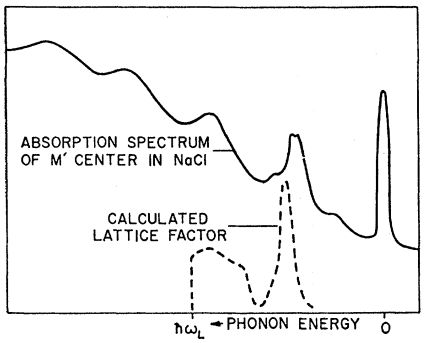

FIG. 9. Absorption spectrum of the NaCl M' center [from Ref. 1(c)] compared to the lattice-factor distribution.

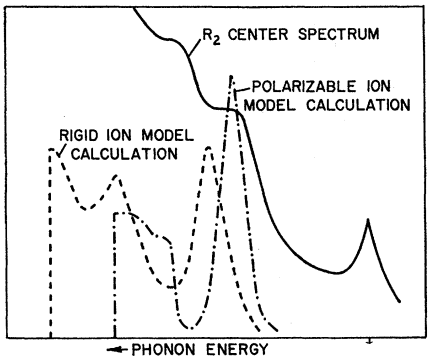

FIG. 10. Absorption spectrum of the NaCl R_2 center [from Ref. 1(b)] and lattice-factor distributions calculated from deformation dipole model ($\hbar\omega_L$=0.03195 eV) and rigid-ion model ($\hbar\omega_L$=0.03954 eV) vibration data.

VI. CONCLUSIONS

Agreement between calculations and experiments have been better than might be expected in view of the restricting approximations employed which have taken into account long-range lattice order but have neglected short-range lattice disorder about an imperfection. The simplifying approximations employed in the theory were: (i) use of a simplifying model of the ionic crystal and neglecting the effects of an imperfection on the lattice dynamics in the electron-lattice interaction; (ii) limitation to explicit consideration of only linear terms in the lattice Hamiltonians, which neglects the eigenvector effect and vibrational frequency differences between the ground and excited states of the electron; (iii) use of nondegenerate electron-states adiabatic-approximation model that neglects effects, such as the Jahn-Teller effect, that may be important. In carrying out the calculations, a further approximation has been made simplifying the dependence of the S_j on the wave functions. For the F-center computations, this was done in forming the F_j factor such that the effects of non-spherical wave functions were neglected. F_j itself was neglected in the one-phonon computations.

The F-band calculations show reasonable agreement with experiments as to the widths of the bands, and the effective frequencies are qualitatively correct in that the emission band is associated with a higher frequency than the absorption band. The latter has a simple interpretation here: The electron in the more diffuse emission states interacts more strongly with the long-wavelength optical modes. In the limit of very diffuse electron wave functions, the interaction is dominated by these modes and the longitudinal-optical-modes approximation applies. To arrive at an effective frequency when the calculations consider many frequencies, a constant C is introduced as in Eq. (5.3) so that the $H(T)$ data conforms to a single-frequency model. However, a C from the calculations compares only in approximate magnitude with a C from experiments. This discrepancy may have arisen because the calculations have neglected the temperature dependence of the S_j.

The one-phonon line-shape calculations show agreement with experiment as to the positions of major features in the attendant phonon structure. This is thought to be significant as the calculated line shapes are a weighting of the lattice modes as stipulated by the derived electron-lattice scalar potential.

ACKNOWLEDGMENTS

We thank Dr. S. S. Jaswal and Dr. A. A. Maradudin for supplying lattice vibration calculations, and Dr. C. E. Blount, Dr. H. R. Fetterman, Dr. D. B. Fitchen, Dr. C. B. Pierce, and Dr. R. H. Silsbee for discussions regarding the experimental data. We thank Dr. J. D. Stettler for helpful discussions. One of us (JTR) acknowledges support from a National Science Foundation Teaching Assistants Summer Fellowship, National Aeronautics and Space Administration Traineeship, and the Redstone Arsenal Army Research Laboratory in the period during which the calculations were completed; the United Kingdom Science Research Council gave support during the preparation of the manuscript. He also thanks Professor C. W. McCombie for helpful discussions.